REVIEW

doi:10.1038/nature14504

Pacific western boundary currents and their roles in climate

Dunxin Hu[1], Lixin Wu[2], Wenju Cai[2,3], Alex Sen Gupta[4], Alexandre Ganachaud[5], Bo Qiu[6], Arnold L. Gordon[7], Xiaopei Lin[2], Zhaohui Chen[2], Shijian Hu[1], Guojian Wang[3], Qingye Wang[1], Janet Sprintall[8], Tangdong Qu[9], Yuji Kashino[10], Fan Wang[1] & William S. Kessler[11]

Pacific Ocean western boundary currents and the interlinked equatorial Pacific circulation system were among the first currents of these types to be explored by pioneering oceanographers. The widely accepted but poorly quantified importance of these currents—in processes such as the El Niño/Southern Oscillation, the Pacific Decadal Oscillation and the Indonesian Throughflow—has triggered renewed interest. Ongoing efforts are seeking to understand the heat and mass balances of the equatorial Pacific, and possible changes associated with greenhouse-gas-induced climate change. Only a concerted international effort will close the observational, theoretical and technical gaps currently limiting a robust answer to these elusive questions.

Western boundary currents (WBCs) are swift, narrow oceanic currents found in all major oceanic gyres. Within the Pacific Ocean, the subtropical gyre WBCs are the Kuroshio Current in the Northern Hemisphere, and the East Australian Current (EAC) in the Southern Hemisphere (Fig. 1a). The Pacific low-latitude, tropical belt WBCs include the Mindanao Current in the Northern Hemisphere and the New Guinea Coastal Undercurrent (NGCUC) south of the Equator, both of which are directly connected to the equatorial Pacific circulation system. Much of modern wind-driven ocean circulation theory was derived from a quest to understand these Pacific Ocean currents. Knowledge of the effect of the Earth's rotation on WBCs, and of the Ekman transport (see Box 1), led to ground-breaking advances: that wind stress (Fig. 1b) is a driving agent of ocean currents, but it is the horizontal gradient rather than the absolute strength that is important; that latitudinal gradients in the effect of Earth's rotation on the horizontal motion cause a flow intensification towards the west of the ocean basins; and that the Pacific wind-forced ocean currents include the equatorial current system, the low-latitude and subtropical WBCs.

Impacts of the Pacific WBCs on the global ocean circulation and climate variability are manifold. First, in winter, the subtropical WBCs are associated with the largest supply of heat and moisture into the atmosphere in the Pacific basin, and are coupled to North Pacific storm tracks[1]. As cold and dry air comes into contact with the warm water carried poleward by the subtropical WBCs, heat and moisture are extracted from the surface. Second, the Indonesian Throughflow (ITF), the only low-latitude inter-ocean current, flows from the Pacific to the Indian Ocean. The throughflow plays a role in the return branch of the global thermohaline circulation[2]. The ITF sources its water mostly from the North Pacific Ocean via the Mindanao Current with the remainder sourced from the South Pacific Ocean via the New Guinea Coastal Current (NGCC), implicating these Pacific WBCs as important players in the global climate system. Third, the Pacific is home to the El Niño/Southern Oscillation (ENSO), the most prominent source of global climate variability on interannual timescales, which severely disrupts global weather patterns, affecting ecosystems, agriculture, tropical cyclones, drought, bushfires, floods and other extreme weather events worldwide[3]. The Pacific low-latitude WBCs are agents for transporting mass into the equatorial Pacific, therefore critically influencing the Western Pacific Warm Pool (a region of sea surface temperatures (SSTs) warmer than 28.5 °C) and the life cycle of ENSO, as well as the East Asian monsoon and the Indian/Southeast Asian monsoon. Finally, the EAC, through its outflow to the Indian Ocean, participates in the Southern Hemisphere supergyre circulation that links the three subtropical gyres[4–6], providing a subtropical gateway for the Pacific's influence on global climate.

Research and observations over the past 15 years have enabled a string of advances in our understanding of the structure of individual components of the Pacific WBCs, interactions amongst them, and their climatic impacts. In particular, several multi-national programmes are underway. Included in these are the Northwestern Pacific Ocean Circulation and Climate Experiment[7], the Southwest Pacific Ocean Circulation and Climate Experiment[8], and the ITF monitoring programme[9], providing an intensive observational focus in Pacific low-latitude regions. These process studies, together with targeted modelling and recent advances in broad-scale sampling of ocean temperature and salinity, upper oceanic currents, winds, precipitation and sea surface heights, as well as satellite retrievals, have led to a significant advance in our understanding of the physical structure and dynamics of the Pacific WBCs, and their possible changes under greenhouse warming.

Here we review the current state of understanding of the structure and variability of the Pacific WBCs, their climatic impacts, and how they may be affected by greenhouse warming. We show that the entire Pacific WBC system moves northwards or southwards concurrently, on seasonal and interannual timescales. The climatic impacts of the Pacific

[1]Key Laboratory of Ocean Circulation and Waves, Institute of Oceanology, Chinese Academy of Sciences, Qingdao 266071, China. [2]Physical Oceanography Laboratory, Qingdao Collaborative Innovation Center of Marine Science and Technology, Ocean University of China, Qingdao 266003, China. [3]CSIRO Oceans and Atmosphere Flagship, Aspendale, Victoria 3195, Australia. [4]Australian Research Council (ARC) Centre of Excellence for Climate System Science, Mathews Building, The University of New South Wales, Sydney 2052, Australia. [5]Institut de Recherche pour le Developpement (IRD), UMR5566-LEGOS, UPS (OMP-PCA), 31400 Toulouse, France. [6]Department of Oceanography, University of Hawaii at Manoa, 1000 Pope Road, Honolulu, Hawaii 96822, USA. [7]Lamont-Doherty Earth Observatory, Earth Institute at Columbia University, Palisades, New York 10964, USA. [8]Scripps Institution of Oceanography, 9500 Gilman Drive, La Jolla, California 92037, USA. [9]IPRC, Department of Oceanography, SOEST, University of Hawaii, Honolulu, Hawaii 96822, USA. [10]Center for Earth Information Science and Technology, Japan Agency for Marine-Earth Science and Technology (JAMSTEC) 3173-25 Showa-machi Kanazawa-ku, Yokohama 236-0001, Japan. [11]NOAA/Pacific Marine Environmental Laboratory, Seattle, Washington 98115, USA.

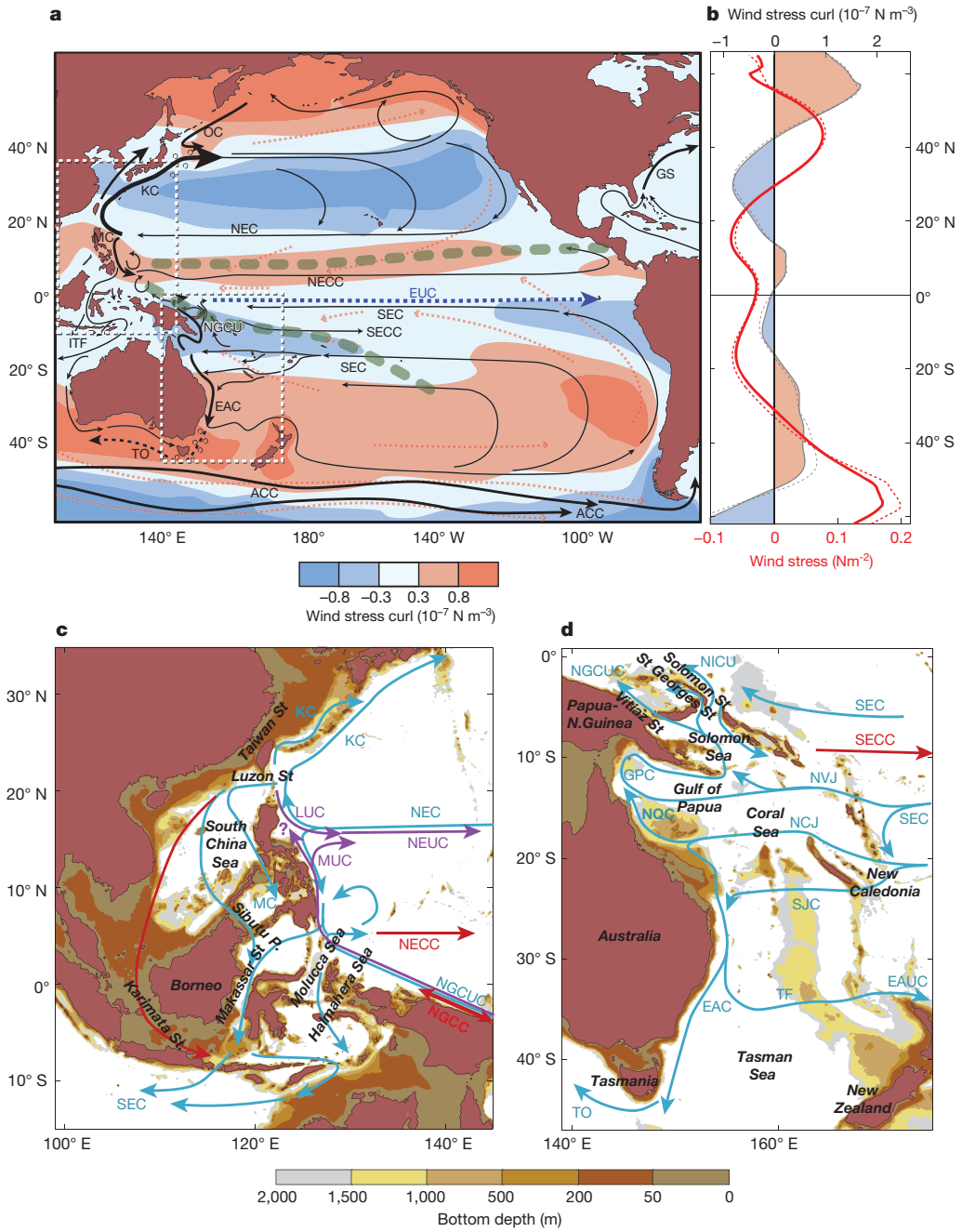

Figure 1 | Pacific Ocean circulation and boundary currents. **a**, Schematic of major currents and observed surface wind vectors (orange dashed lines) and wind stress curl (shading: positive curl in red; negative in blue). The Intertropical Convergence Zone and the South Pacific Convergence Zone are indicated by thick grey-dashed lines. Red and blue shading in the Southern Hemisphere corresponds to anticyclonic and cyclonic curls, respectively, and vice versa in the Northern Hemisphere. **b**, Pacific zonally averaged zonal wind stress (grey curve) and wind stress curl (red curve) for the present day (solid lines) and the latter half of the twenty-first century (dashed lines). Projected changes are calculated as the multi-model mean difference between 2050–2100 future winds under RCP8.5 and 1900–2000 historical winds. OC, Oyashio Current; KC, Kuroshio Current; NEC, North Equatorial Current; MC, Mindanao Current; NECC, North Equatorial Counter Current; NEC, North Equatorial Current; EUC, Equatorial Undercurrent; NGCUC, New Guinea Coastal Undercurrent; ITF, Indonesian Throughflow; SECC, South Equatorial Counter Current; SEC, South Equatorial Current; EAC, East Australian Current; TO, Tasman Outflow; ACC, Antarctic Circumpolar Current; GS, Gulf Stream. **c**, **d**, Topographic and boundary current systems in the Northwest Pacific (**c**) and Southwest Pacific (**d**), as indicated by the dashed white boxes in **a**. Depths shallower than 2,000 m are colour-shaded. Grey shading indicates depths shallower than 50 m. The main currents, integrated from 1,000 m to the surface, are indicated by light blue arrows; the red curved arrow indicates the 'freshwater plug'; red straight arrows indicate the main surface-trapped counter currents; purple arrows indicate undercurrents; question mark indicates uncertainty in flow path. Panel **c** is adapted from ref. 8 (John Wiley and Sons). LUC, Luzon Undercurrent; MUC, Mindanao Undercurrent; NGCC, New Guinea Coastal Current; NEUC, North Equatorial Undercurrent; NICU, New Ireland Coastal Current; NVJ, North Vanuatu Jet; NCJ, North Caledonia Jet; SCJ, South Caledonia Jet; NQC, North Queensland Current; GPC, Gulf of Papua Current; TF, Tasman Front; EAUC, East Auckland Current; TO, Tasman Outflow.

WBCs are far-reaching, and are exerted in many ways, including through interactions with the South China Sea circulation, the Tropical Pacific Warm Pool, and the ITF; through longevity of SST anomalies along the WBCs and their feedback to the atmosphere; and through contribution to the global thermohaline circulation. Under greenhouse warming, the response of Pacific WBCs is uncertain, although changes are not expected to resemble anomalies associated with climate variability.

BOX 1

Processes associated with the Pacific surface WBCs

Ekman transport and oceanic currents. In the tropical Pacific, the main currents, westward flowing over the upper ocean, are forced by the easterly trade winds. In the first few tens of metres of water depth, immediately away from the Equator, deflection by the rotation of the Earth occurs to the right in the Northern Hemisphere, and left in the Southern Hemisphere. This 'Coriolis' force causes 'Ekman transport', whereby tropical surface waters move poleward in both hemispheres. Likewise, poleward of 25° N and 25° S, the prevailing westerly winds induce Ekman transports towards the Equator, generating a convergence between 15°–30° N and 15°–30° S, with high sea levels around 10°–15° N and 10°–15° S, respectively. The sea-level slope drives two broad geostrophic westward flows: the North Equatorial Current (NEC) and the South Equatorial Current (SEC).

Bifurcation and WBCs. Upon approaching the western boundaries, equatorial currents split into two branches: equatorward low-latitude WBCs; and poleward subtropical WBCs. In the Pacific, the NEC bifurcates into the equatorward Mindanao Current and the poleward Kuroshio Current, and the SEC bifurcates into the equatorward Gulf of Papua Current and poleward East Australia Current (EAC).

Rossby wave adjustment. The above ocean wind–current relationship assumes a steady wind forcing the ocean for a long time. Winds vary on the large scale, and the ocean adjusts by generating large-scale anomalies that move in the form of oceanic Rossby waves. Such waves propagate along the thermocline, a boundary between the warm upper layer and the cold deeper part of the ocean, and always propagate westward because of the latitudinal gradient of the tangential speed of the Earth's rotation.

Wind stress curl. It is not the absolute magnitude of the wind stress but rather its curl (the horizontal gradient of the stress) that forces the north–south transport of the interior ocean. At some locations, the curl is reduced to zero and there is no north–south transport (although there might be flows at depth which cancel when summed up). Lines along which the curl is zero provide natural boundaries that separate circulation into gyres. Such lines in subtropical latitudes are often used as an approximation to locate the bifurcation latitude.

Kuroshio Extension. At some latitude, the Kuroshio Current separates from the coast and flows eastward into the ocean interior. At this eastward excursion, the Kuroshio Extension has some of the largest air–sea fluxes found across the North Pacific basin. It is a region with a great quantity of latent, sensible, and net surface heat loss, and is co-located with the Pacific storm track.

Tasman Front and Tasman Outflow. In the South Pacific, part of the EAC separates from the coast and veers eastward as the Tasman Front; the residual continues southward passing through the Tasman Sea. A portion of the Tasman Front attaches to the northern coast of New Zealand, forming the East Auckland Current. The portion flowing through the Tasman Sea reaches Tasmania and turns westward into the eastern Indian Ocean as Tasman Outflow.

Structure of the Pacific WBC system

Driven by the large-scale pattern of wind stress curl (see Box 1), the Pacific WBC system is characterized by the unique presence of two intense equatorward WBCs—the Mindanao Current and the NGCUC. These serve as subtropical-to-tropical oceanic pathways that modulate the mass and heat balances of the Western Pacific Warm Pool, and the ventilation of the equatorial Pacific thermocline. As such, low-latitude WBCs are a part of the life cycle of ENSO and Pacific decadal variability[10,11].

The Mindanao Current and the NGCUC originate at the bifurcations of zonal currents arriving at the western boundaries: the westward-flowing North Equatorial Current (NEC) in the North Pacific, and the South Equatorial Current (SEC) in the South Pacific. Upon reaching the Philippine coast, the NEC bifurcates to feed the poleward Kuroshio Current[12] and the equatorward Mindanao Current[13] (Fig. 1c). In a similar manner, the westward-flowing SEC bifurcates at the Australian coast into the northward-flowing Gulf of Papua Current[14] and southward-flowing EAC[15]. The Gulf of Papua Current feeds the NGCUC, which exits through narrow straits at the northern boundary of the Solomon Sea[16], connecting the South Pacific to the Equator and the ITF (Fig. 1c, d).

The convergence of the Mindanao Current and NGCUC near the Equator (Fig. 2) feeds the Western Pacific Warm Pool, the surface to lower thermocline of the ITF[17], and the eastward-flowing Equatorial Undercurrent (EUC)[18]. In this way, the two low-latitude WBCs together with the strong mixing in the Indonesian Seas largely determine the water mass characteristics of the Pacific equatorial current systems and of the ITF[18]. Also involved in the mass balance of the Western Pacific are counter currents, which are associated with the Intertropical Convergence Zone and the South Pacific Convergence Zone, the two prominent rainbands in the Pacific. These convergence zones themselves, together with local winds they have altered and the associated wind stress curl, produce two eastward-flowing, surface-intensified counter currents, known as the North Equatorial Counter Current[19] and the South Equatorial Counter Current[20] (Fig. 1a).

The Pacific low-latitude current system has a rich vertical structure, and over the years there has been conflicting evidence as to the nature of some currents[21–29]. In both hemispheres, the bifurcation latitude increases with depth. For example, the long-term average NEC bifurcation latitude is approximately 14° N at the surface, but 20° N at a depth of 1,000 m. The Luzon Undercurrent[22,23], observed beneath the Kuroshio, with a core at depths around 650 m near 18° N, intensifies towards the south before turning to the east to feed the North Equatorial Undercurrent. By contrast, despite the suggestion of a northward-flowing Mindanao Undercurrent with a centre at around 600 m (refs 21, 24–26; Fig. 2a), debate persisted as to whether it is transient in nature[27], a quasi-permanent flow but affected by thermocline variability[28], or a subthermocline eddy[29]. The presence of the undercurrent at depths below 400 m has been confirmed by recent measurements (Fig. 2a; ref. 25).

In the South Pacific, the range of the SEC bifurcation latitudes as a function of depth is large, varying between 13° and 25° S. The surface SEC flow turns southward feeding the EAC, while the subsurface flow, the Great Barrier Reef Undercurrent (part of the Gulf of Papua Current system), veers northward feeding the NGCUC[20–32]. The Great Barrier Reef Undercurrent, the South Pacific counterpart of the Luzon Undercurrent, has been linked to the basin-scale circulation of the subtropical gyre that contracts poleward with depth[33]. The NGCUC was recently measured[31] as a strong, permanent undercurrent against the coast of Papua New Guinea (Fig. 2b), with its core at about 400 m carrying the bulk of the South Pacific low-latitude WBC transport that splits in the different Solomon Sea straits then flows towards the Equator or the ITF[8].

Because the seasonal wind stress curl variability that controls the bifurcation latitude is due to seasonal movement of trade winds, the NEC and SEC bifurcations move synchronously and in the same meridional direction on seasonal timescales. At the surface, the NEC bifurcation latitude moves from 15° N in boreal summer, to 17° N in boreal winter[34], in conjunction with the seasonal reversal of the South East Asia monsoon. This seasonal movement is accompanied by a stronger NEC leading to both a stronger Mindanao Current and Kuroshio Current when the bifurcation occurs at lower latitudes in boreal summer, increasing the tropical water injection into the North Pacific subtropical gyre[13]. As such, the NEC, the Mindanao Current and the Kuroshio Current transport east of Luzon are all at their seasonal maximum during boreal summer (June–July) when bifurcation occurs at the southernmost latitude[34,35] but minimum during boreal winter (November–December) when bifurcation occurs at the northernmost

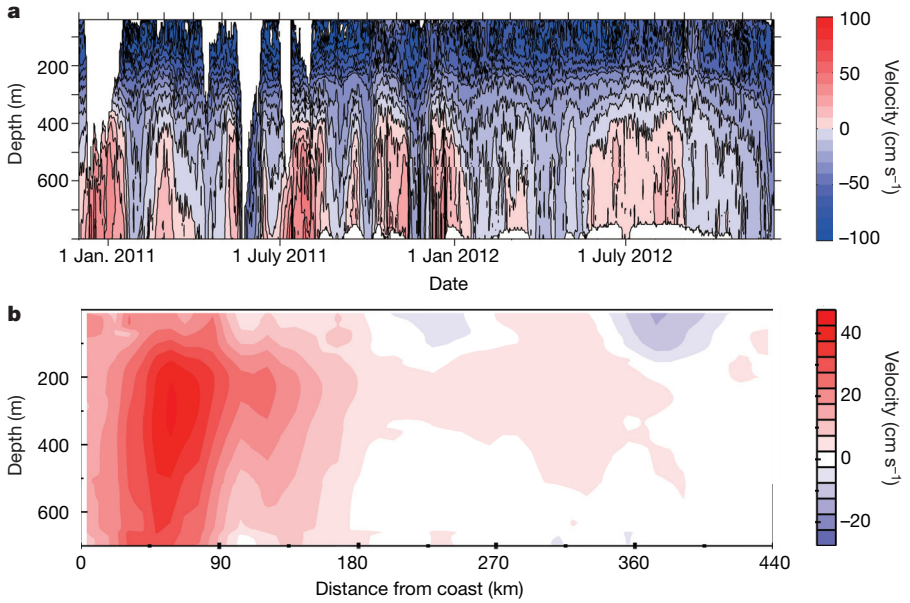

Figure 2 | Characteristics of the two equatorward low-latitude WBCs in the tropical Pacific. Such WBCs are a unique feature of the Pacific Ocean. **a**, Moored current meter data at 8° N, 127° E showing evolution of meridional velocities, the Mindanao Current (blue, negative values) and its undercurrent (red, positive values) from boreal winter 2010 to boreal winter 2012, adapted from ref. 26 (John Wiley and Sons). Shown are daily ADCP data smoothed by a three-day running mean filter. Moorings were anchored in 6,100 m deep water, with two 75K RDI ADCP current meters at ~400 m scanning up and down, respectively. The current meters move vertically in the water column, as strong currents interact with the mooring system. **b**, Velocity section across the South Solomon Sea, from a compilation of glider observations adapted from ref. 31 (AMS). Units are cm s^{-1}. Red shading indicates equatorward flow, and blue poleward flow. The NGCUC is characterized by a strong core, centred at about 400 m, against the coast of Papua New Guinea, to the left of the section. The *x*-axis represents an equivalent eastward distance from the coast of Papua New Guinea.

latitude. The SEC bifurcation shifts northward towards the Equator in austral summer (November–December), and is southernmost in austral winter (June–July)[15]. When the SEC is closer to the Equator, its transport strengthens, feeding more water into both the EAC and the NGCUC[15]. The EAC attains a maximum transport (up to 36 Sv; 1 Sv = 10^6 m^3 s^{-1}) and extends furthest poleward in austral summer with a large Tasman Outflow into the Indian Ocean. In austral winter, the EAC transport weakens (to 27 Sv), and much of this veers eastward as the Tasman Front (Fig. 1d; ref. 36).

Consistent with dynamical argument, observations have shown that the South Pacific subtropical gyre and the Tasman Outflow south of Australia are part of a system of nested anticyclonic gyres encompassing the entire Southern Hemisphere subtropics, connecting the Atlantic, Indian and Pacific basins to the global thermohaline circulation[4–6,37,38]. The Atlantic and Indian Oceans are connected south of Africa by a westward Agulhas leakage and the eastward South Atlantic Current[38], while the Pacific and Indian Oceans are connected south of Tasmania by the westward Tasman Outflow[4,5,37], a narrow boundary flow of the western Pacific gyre that turns westward around the south of Tasmania and 'leaks' to the Indian Ocean basin[4]. Tasman leakage occurs primarily as a subsurface or intermediate water circulation[6], in contrast to the ITF route that largely occurs in the upper 300 m. The linkage of the Tasman leakage to the supergyre provides a mechanism whereby Antarctic Intermediate Water, which transits to the southwest Pacific, is distributed between the ocean basins before it spreads northward into the Pacific, Indian and Atlantic oceans[5,6].

Variability of the Pacific WBCs

Pacific WBCs are subject to strong variability on intraseasonal[26,27,39], interannual[30,40–44], decadal and longer timescales[42,43]. However, as a result of possible eddy aliasing[30,44], and the discrete short-term nature of *in situ* surveys that may be difficult to place in an appropriate climate context, there is large uncertainty in the volume transport estimate of these WBCs. For example, the Mindanao Current transport ranges from 13 to 39 Sv depending on the study[12,27,41].

The NEC bifurcation latitude and its partitioning into the Mindanao Current and the Kuroshio Current are affected by many factors, including local monsoonal winds and buoyancy fluxes, and remote forcing from the Pacific interior and North Pacific along the western boundary[35,40]. The main forcing, though, is ENSO. The response of the WBCs to ENSO, in turn, influences the life cycle of ENSO. As an El Niño develops, the entire Pacific circulation system 'breathes' together, bifurcating at a more northerly latitude (Fig. 3a, b), as manifested through a positive correlation of ENSO with the north and south bifurcation latitudes. Accompanying the more northerly bifurcation are a stronger NEC and North Equatorial Counter Current, a stronger Mindanao Current, a more intense EUC at its westernmost part, but a weaker Kuroshio Current and ITF[28,30,40] (Fig. 3a). To the south, the NGCUC intensifies during, or several months after, the peak of an El Niño[30], and the surface southward NGCC disappears and turns northwards (Fig. 3b), as occurred from July to February during the 1997–98 extreme El Niño[45]. Although the EAC transport displays variability on interannnual timescales, only a weak ENSO signal is evident in observations[36].

The responses of the Mindanao Current and the NGCUC to ENSO as described above are integral to the ENSO discharge/recharge cycle[46]. The increased equatorward WBC transport during an El Niño creates a strong confluence of relatively cooler water in the tropical western Pacific, and constitutes a compensatory flow for the associated discharge of the equatorial Pacific warm water, conducted in the interior Pacific through the Sverdrup process, whereby mass is pumped out of the equatorial west Pacific in response to wind forcing.

Recent observations revealed a rich spatial structure and a large response of the SEC transport to ENSO[30–32]. Variability of the NGCUC inflow to the Solomon Sea can reach 100% of the mean transport, with the changes mainly occurring in the upper 250 m. During an El Niño event, the SEC transport between New Caledonia and the Solomon Islands increases[21,31,32], particularly in the North Vanuatu Jet, with an enhanced transport entering the Solomon Sea (Fig. 3b). This leads to an increased equatorward mass transport through the Solomon Strait and

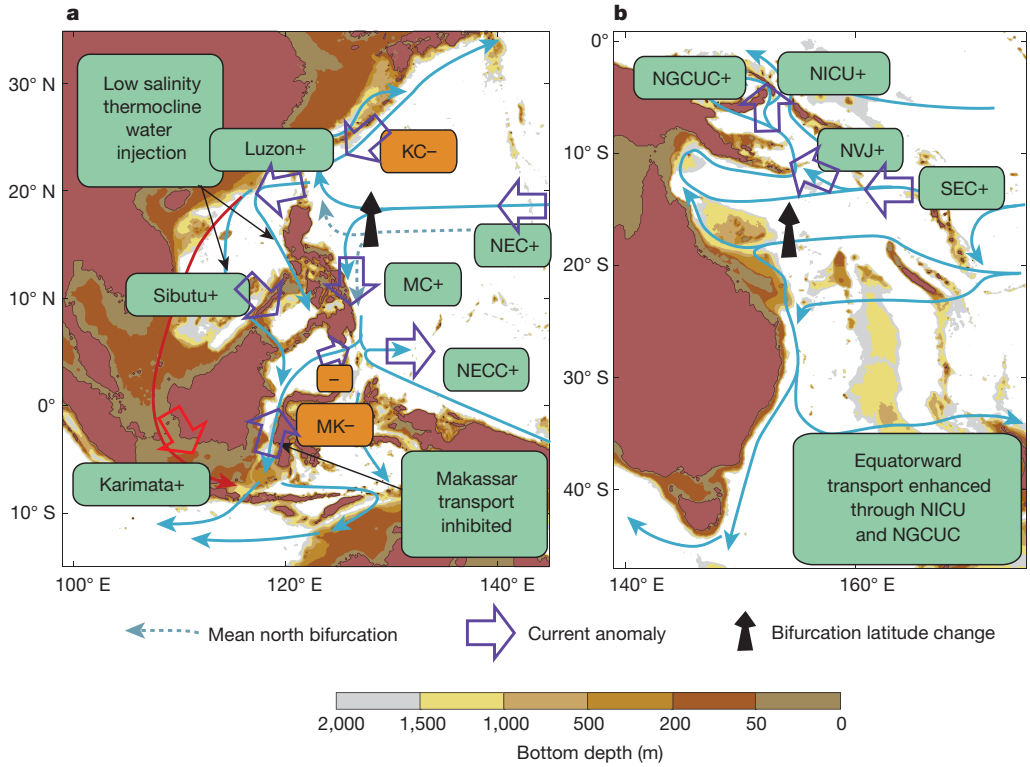

Figure 3 | Impact of El Niño on the Pacific WBC system. **a**, **b**, During an El Niño, the bifurcation moves north in both the Northern (**a**) and the Southern (**b**) Hemispheres, as indicated by the black arrows. The ocean depth is indicated as on Fig. 1c, d. Increasing (green boxes) and decreasing (orange boxes) flow anomalies during El Niño are indicated. Some currents are enhanced, while others are weakened, as indicated by the anomalies (large dark blue/red arrows). From the developing phase to approximately three-to-four months before the peak of an El Niño, the Kuroshio Current (KC) decreases while the Mindanao Current increases. The ITF weakens as the Pacific-Indian pressure gradient reduces. The South China Sea Throughflow intensifies, setting up a freshwater plug. Towards the peak of an El Niño, equatorward transport enhances through NICU and NGCUC. LUC, Luzon Undercurrent; MUC, Mindanao Undercurrent; NGCC, New Guinea Coastal Current; NEUC, North Equatorial Undercurrent; NICU, New Ireland Coastal Current; NVJ, North Vanuatu Jet; NCJ, North Caledonia Jet; SCJ, South Caledonia Jet; NQC, North Queensland Current; GPC, Gulf of Papua Current; TF, Tasman Front; EAUC, East Auckland Current; TO, Tasman Outflow.

through the New Ireland Coastal Undercurrent, in addition to the increased transport via the Vitiaz Strait[45,47] (see Fig. 3b). The transport of heat and salt through the Solomon Sea can change by up to a factor of two between extreme El Niño and La Niña conditions[47].

Connections between the Pacific WBCs and the ITF are complex, particularly when ENSO is considered. Synthesis of observational data and model simulations indicates that the depth and velocity of the ITF core vary with ENSO, with the ITF slowing and shoaling during El Niño events[48]. Modelling and observational studies indicate that, on average, the proportion of the ITF water derived from the North and South Pacific depends sensitively on ENSO phases. Climatologically, approximately 80% of the ITF originates from the North Pacific and 20% from the South Pacific via the NGCUC[48–50]. As a La Niña develops, the ITF increases due to stronger easterly trade winds, which induces a pressure gradient between the West Pacific and the eastern Indian Ocean. Climate models suggest a greater amount of ITF water originates from the South Pacific during La Niña compared to during El Niño[49]. During the development of La Niña, a seasonal and ENSO-dependent inflow from the Luzon Strait to the Indonesian Seas forced by large-scale winds in the Pacific, called the South China Sea Throughflow[51], weakens. Further, the Mindanao Current transport decreases, though a greater portion of this current goes into the ITF at the expense of the North Equatorial Counter Current[50].

Interactions between the Pacific WBCs and the Pacific Decadal Oscillation (PDO) occur on decadal timescales in a manner somewhat different to the interannual timescales for ENSO, particularly in the North Pacific[42,43]. The post-1990 cold PDO phase is linked to a southward shift of the NEC bifurcation latitude, and a strengthened NEC and North Equatorial Counter Current, as a result of intensified easterlies over the Western Pacific[42,43]. Both the Kuroshio Current and the Mindanao Current have also strengthened, inconsistent with ENSO-induced changes, which would imply a decreased Mindanao Current. In the Southern Hemisphere, observations and ocean reanalysis suggest that a cold phase of the PDO is associated with a deeper southward EAC extension[36], while the Tasman Front weakens, which suggests that there is a gating between these two currents[52]. In the two decades before 1993, the PDO was in a warm phase, whereby the trade winds across the tropical Pacific were weaker, consistent with a weaker atmospheric Walker circulation[53]. In response, the NEC and its counter currents were also weaker and shifted northward[42,43].

Multidecadal fluctuations can also modulate the interannual relationship between ENSO and the NEC bifurcation latitude, such that the relationship between ENSO and the northwestern Pacific WBCs is non-stationary[13,43]. The NEC mean bifurcation latitude is situated further to the south during a cold PDO phase, and from this more southward position the NEC bifurcation latitude can 'jump' a considerable distance to the north during an El Niño. As such, interannual NEC bifurcation variability is more strongly correlated to the Niño-3.4 index during the cold phase of the PDO. Thus, the bifurcation latitude of the NEC which is determined by wind forcing in the 12°–14° N band also contains variability not solely represented by the Niño-3.4 index[42].

Interactions with climate

The Pacific WBCs interact with physical climate on synoptic, interannual and long-term climate scales, and such interactions are better understood for the North Pacific than for the South Pacific. In boreal winter, strong advection of warm water by the Kuroshio Current into regions of

colder air temperatures, such as the Kuroshio/Oyashio extension region, results in large losses of latent and sensible heat to the atmosphere[54,55]. This heat loss triggers oceanic and atmospheric deep convection, and fuels storms for their recurrent development, while contributing to the formation of mode waters[55]. In the mixed water region north of the Kuroshio Extension, turbulent heat fluxes of more than 600 W m^{-2} are observed during wintertime northerly wind events[56], where the contrast between the WBC warm core and adjacent waters gives rise to particularly large SST gradients: more than 10 °C over 200 km across the Oyashio Front. The presence of such oceanic fronts can generate atmospheric instability, and increased vertical momentum exchange, as well as winds induced by changes in air density[57,58]. This tends to exert a positive feedback, whereby larger turbulent heat fluxes from the ocean to the atmosphere over the warm core of the current generate even stronger winds[57,58]. Atmospheric eddy heat fluxes associated with synoptic systems act to reduce the sharp meridional air temperature gradients[1], but the large thermal inertia of the ocean mixed-layer and oceanic advection rapidly restore the SST front and the air temperature gradient[59]. An impact of the warm water maintained in this manner is that typhoons tend to strengthen as they pass over the warm core of the Kuroshio Current[60]. During summer time, heat and moisture supply from the warm Kuroshio, though less than in winter, is effective in retaining the convectively unstable stratification of low-level northwestward monsoonal airflow from the tropics, enhancing the convective heavy rainfall along the Kuroshio[61].

Beyond synoptic scales, the North Pacific WBCs exert a considerable impact on Asia summer monsoons[62,63]. One such impact is on the South China Sea summer monsoon, which marks the commencement of the Asia summer monsoon. In post-La Niña boreal spring and early summer, the western tropical Pacific heat content is anomalously high, as a part of the heat recharge associated with stronger trade winds. In association with a stronger Walker circulation, convection over the eastern Indian Ocean and the Western Pacific remains strong, resulting in stronger-than-normal westerlies over the tropical Indian Ocean delivering the crucial moisture source favourable for the South China Sea summer monsoon[63]. Consequently, the South China Sea summer monsoon commences earlier than normal, leading to droughts along the middle-lower Yangtze River basin and floods in southern and northern China[61]. Thus, the heat content of the Western Pacific Warm Pool can be a predictor of the South China Sea summer monsoon onset and strength, with a high heat content associated with an early onset and strong intensity[63]. Conversely, in the late boreal spring-early summer after an El Niño, when the warm pool is still cooler than normal, the South China Sea monsoon takes place later than normal, causing floods along the middle-lower Yangtze River basin and drought in southern and northern China[63]. A similar link exists between the Australian summer monsoon and ENSO via SST anomalies in the central and Western Pacific[64]; however, the timing is different. The Australian summer monsoon tends to be weakened, concurrently, by an El Niño, and strengthened by a La Niña.

Interactions between the North Pacific WBCs and the South China Sea Throughflow[65] on seasonal and interannual timescales constitute another source of climatic influence. During the boreal winter, when the northwest monsoon prevails over the Indonesian Seas, or during El Niño periods, the wind drives buoyant, low-salinity surface water derived from the South China Sea via the Karimata Strait (Fig. 1c) into the southern Makassar Strait[65] and from the Sibutu Passage into the northern Makassar Strait[50]. This creates an anomalous pressure gradient in the surface layer of the Makassar Strait (red curved arrow, Fig. 1c) that inhibits the warm surface water from the Mindanao Current from entering into the ITF. This surface-layer 'freshwater plug', originally due to heavy rainfall and large runoff from Southeast Asia, inhibits the Pacific warm surface water from flowing southward into the Indian Ocean, leading to a reduced, cooler ITF in the Makassar Strait during December–January and during El Niño, and inducing a cooler upper Indian Ocean, which may in turn weaken the Asian monsoon[65]. During the boreal summer, when winds in the Indonesian Seas reverse to the southeast monsoon, or during La Niña periods, the obstructing pressure gradient is reduced, reducing the impact of the freshwater plug, supporting an earlier and stronger South China Sea monsoon in the late spring, or early summer after a La Niña event[50].

Variations in the North Pacific WBCs also exert a climatic impact through the longevity of SST anomalies they generate[54,55,66–70], influencing the large-scale atmospheric circulation and storm-track activities, particularly near the multiple fronts of the WBC extension[1,71,72]. These extension fronts are fertile grounds for strong SST variability. Because of the strong horizontal gradients, a slight frontal movement can lead to a large change in SSTs and is an effective process for generating SST variability[66,69]. Frontal movement can be generated by intrinsic variability of the WBCs as well as by remote ocean and atmosphere forcing via extratropical ocean Rossby waves[67–70]. The Kuroshio Extension fronts, for example, are strongly influenced by large-scale changes in the subtropical gyre driven by wind stress changes across the North Pacific[42,73], and by ENSO-induced basin-scale wind stress curl anomalies through atmospheric teleconnections[67,68], emanating from the tropical Pacific, remotely forcing SST variability in the Kuroshio Extension region via oceanic Rossby waves[73,74].

The longevity of SST anomalies along the Kuroshio Extension can be further enhanced by processes that either maintain or reinforce the anomalies[75–80]. For example, in boreal summer, the North Pacific Ocean cools the warm moist air advected from the south, inducing the formation of low-level stratus and fog within the boundary layer on the northern sides of the Kuroshio Extension fronts[75,76]. These clouds (in particular low clouds) reduce solar insolation because of their high albedo, in turn maintaining low SSTs[76,77]. This positive 'cloud–SST feedback' acts to reinforce cold SST anomalies, and can enhance and prolong summertime cold SST anomalies near the North Pacific subarctic front zone[78]. In boreal winter, through anomalous geostrophic heat advection, the axial migration of the Kuroshio Current and the associated frontal movement generate subsurface temperature anomalies that can persist over multiple years. Shoaling of the North Pacific mixed layer in boreal spring and deepening in autumn results in mid-latitude SST anomalies recurring from one winter to the next without persisting through the intervening summer[79,80]. This 're-emergence mechanism' operates when SST anomalies spread throughout the deep winter mixed layer, but remain beneath the mixed layer in spring, isolated from the 'damping' surface fluxes. When the mixed-layer deepens again in the following autumn, the temperature anomalies are brought out into the surface layer and influence SST[80]. Along the Kuroshio Extension, advection by the mean currents transports these anomalies by as much as 4,000 km over the course of a year[79,80]. These processes are favourable for decadal SST variability such that it is particularly strong along such fronts[55,69,81].

Climatic impacts of the EAC are less well understood, but there is suggestion of an influence on Australian and New Zealand climates. Weaker EAC transport is linked to anomalous cool conditions in New Zealand[82], and a stronger EAC is shown to promote rainfall along the east Australia coast[83]. However, little is known about the impact of the EAC on, for example, storm tracks or atmospheric circulations.

The Pacific WBCs exert substantial influence on timescales longer than decadal, and on climate remote from the Pacific regions, through their linkage to the Southern Hemisphere supergyre circulation via the Tasman Outflow[4–6,38] and the ITF[9,48,84–87]. The Tasman Outflow influences downstream ocean climate through intermediate-depth water[4], but the influence through the ITF is conducted through the upper 300 m (ref. 9). Increased transport within the warmer upper layer of the ITF modifies the heat budget of the Indian Ocean[84,85] as well as the residence time of tropical Indian Ocean waters[86], thermocline depth and SST patterns[87]. Further downstream, the ITF feeds the Agulhas leakage, and ultimately provides an important heat source for supporting the global thermohaline circulation[2].

Observed changes and future projection

Over the past century, there has been direct and indirect evidence supporting changes having occurred in the subtropical gyres. For example, there appears to be a synchronous surface ocean warming along the path of all subtropical WBCs that is two-to-three times greater than the global mean[88]. The enhanced warming is associated with a poleward shift and/or intensification of global subtropical WBCs in conjunction with a systematic change in winds over both hemispheres. Specifically, the zero-curl line shifted poleward in the North Pacific, the North Atlantic and the South Atlantic Oceans; in the South Pacific and South Indian Oceans, high-latitude westerly winds strengthened while mid-latitude southeasterly trade winds weakened[5,37], consistent with a positive trend of the Southern Annular Mode[5,38], leading to accelerated warming and an intensified supergyre.

Over the past 60 years, there has been a synchronous long-term southward shift of the NEC and the SEC bifurcations[89] in the tropical Pacific (Fig. 4a, b), similar to their synchronous movement on interannual timescales. Over the 60-year period, the overall long-term southward shift of the NEC is modulated by a slight northward migration from 1970 to 1992 (ref. 90) and a southward shift in the post-2000 period, associated with the warm and cold PDO phases, respectively. The long-term southward shift of the latitude of the NEC bifurcation suggests a strengthening Kuroshio Current, consistent with the observed accelerated warming (Fig. 4a). By contrast, the southward shift of the SEC bifurcation has no bearing on the transport partition, but is accompanied by a substantial southward extension of the EAC[5,37]. The relative importance of greenhouse warming and decadal variability for the North Pacific changes is difficult to quantify. However, about two-thirds of the poleward intensification of the Southern Hemisphere supergyre circulation, including the southward EAC extension and the strengthening of the Tasman Outflow[91,92], has been attributed to wind changes induced by Antarctic ozone depletion[93], and one-third to increasing atmospheric CO_2 (refs 91–93).

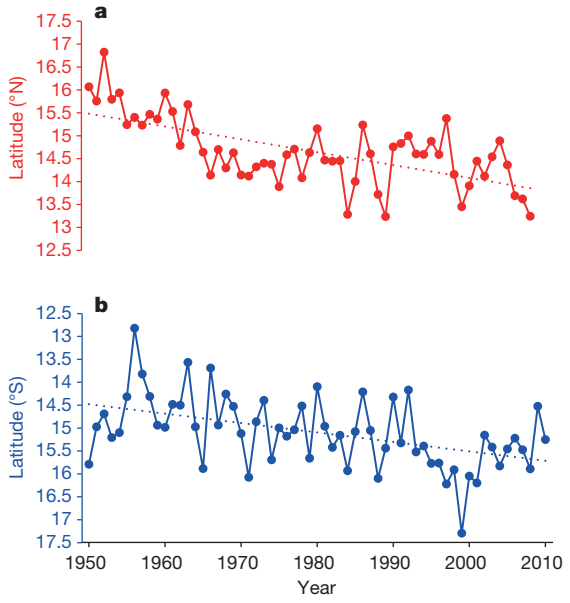

Figure 4 | Trend in the bifurcation latitude of the North and South Equatorial Currents. **a**, **b**, Time series of annual mean NEC bifurcation latitude integrated over the upper 381 m (**a**; red curve, adapted from ref. 90 (John Wiley and Sons)), and of SEC bifurcation latitudes integrated over the upper 200 m (**b**; blue line, adapted from ref. 89 (John Wiley and Sons)), based on SODA version 2.2.4. The bifurcation in each layer of SODA data is defined as where the meridional velocity averaged within a 2° longitude band off the Philippine/Australian coast is zero. Correlation between the NEC bifurcation latitude and Niño-3.4 is $r = 0.55$, and between the SEC bifurcation latitude and Niño-3.4 is $r = 0.40$, both statistically significant above the 95% confidence level. Both trend lines are above the 95% confidence level.

Projected changes in the Pacific WBCs depend on emission scenarios of greenhouse gases. Antarctic ozone is projected to recover by around the middle of this century, providing a mechanism to offset the impacts of a projected continuous increase in CO_2. As such, climate models under the business-as-usual emission scenario, which currently matches the observed emission rates, simulate no further trend in the Southern Hemisphere westerly winds before 2045, but an acceleration in the post-2045 period[94]. In the following two paragraphs, we discuss projected changes averaged over the 2050–2100 period referenced to the mean conditions over the twentieth century, under this emission scenario.

Climate models consistently indicate that the Tasman Outflow transport will continue to increase (from ~2 Sv in the twentieth century to ~6 Sv over 2050–2100) and that the latitude of maximum EAC transport will shift further south (~1.5° latitude over 2050–2100; ref. 94); however, the projected EAC maximum transport shows little change (Fig. 5). In the North Pacific, the Kuroshio Current is projected to weaken at its origin by approximately 10%, although the maximum Kuroshio transport shows little change. The EUC tends to strengthen in the eastern and central Pacific (Fig. 5) and become shallower, particularly in the west[95,96]. This tendency for strengthening occurs despite a weakening of the equatorial trade winds[53]. The projected EUC intensification is driven by a projected strengthening of the NGCUC that results from a wind stress curl change that is negative, associated with a weakening of the equatorial trade winds and a strengthening of the southeasterly trade winds[96]. A strengthening of the NGCUC supporting a strong EUC is consistent with a present-day observation that much of the NGCUC transport goes to support the EUC[97], although the range in model projections is rather large.

Both the Mindanao Current and the ITF are projected to weaken (Fig. 5). The reduced ITF is not fully accounted for by the projected wind-induced changes through Sverdrup dynamics that exclude an influence from upwelling deep water. This exclusion is an invalid assumption because such upwelling is important on timescales relevant for climate change. It is conceivable that a projected slowdown of the global thermohaline circulation[98] would drive a weakening in upwelling of deep water in the South Pacific, contributing to the projected ITF decrease, and following the notion that the ITF is in part supported by the upwelled deep water associated with the compensating flow for the global thermohaline circulation[2].

Uncertain outcome

There is little doubt that the mean climate over the Pacific will continue to change in the coming century owing to past and future emissions of greenhouse gases. Climate models suggest that the tropical trade winds are likely to weaken[53], and that the southern mid-latitude westerlies are likely to undergo a poleward shift and intensification[91–94], and contribute to the intensification of the WBCs, although changes in North Pacific winds are less clear[99]. These changes, together with a projected weakening in the global thermohaline circulation[98], may simultaneously affect the Pacific WBCs. Further, such changes may not resemble anomalies associated with variability on interannual or inter-decadal timescales[96].

Although climate models agree on many aspects of the projected future changes, such as the weakening of the NEC and the NECC and the strengthening of the NGCUC and the NQC, the simulation of WBCs is generally poor because these coarse-resolution simulations do not resolve the terrain of marginal seas, complex flow structure of WBCs, bathymetry and eddies. Certain aspects of future change in high-resolution models remain consistent with the lower-resolution models[100], but uncertainty in projected changes remains high. Another challenge is the lack of information about the flow structure and amplitude of the low-latitude Pacific WBCs in the real world, necessary for benchmarking climate models. For example, despite an extensive observational campaign, the ITF mass budget is not closed; the estimated outflow exceeds the inflow by ~2 Sv (ref. 9). It is unknown whether a contribution from the NGCUC through the Molucca and Halmahera Seas might account for the discrepancy. This mass imbalance is linked to many long-standing issues, including whether Antarctic Intermediate Water, through the NGCUC and the Mindanao

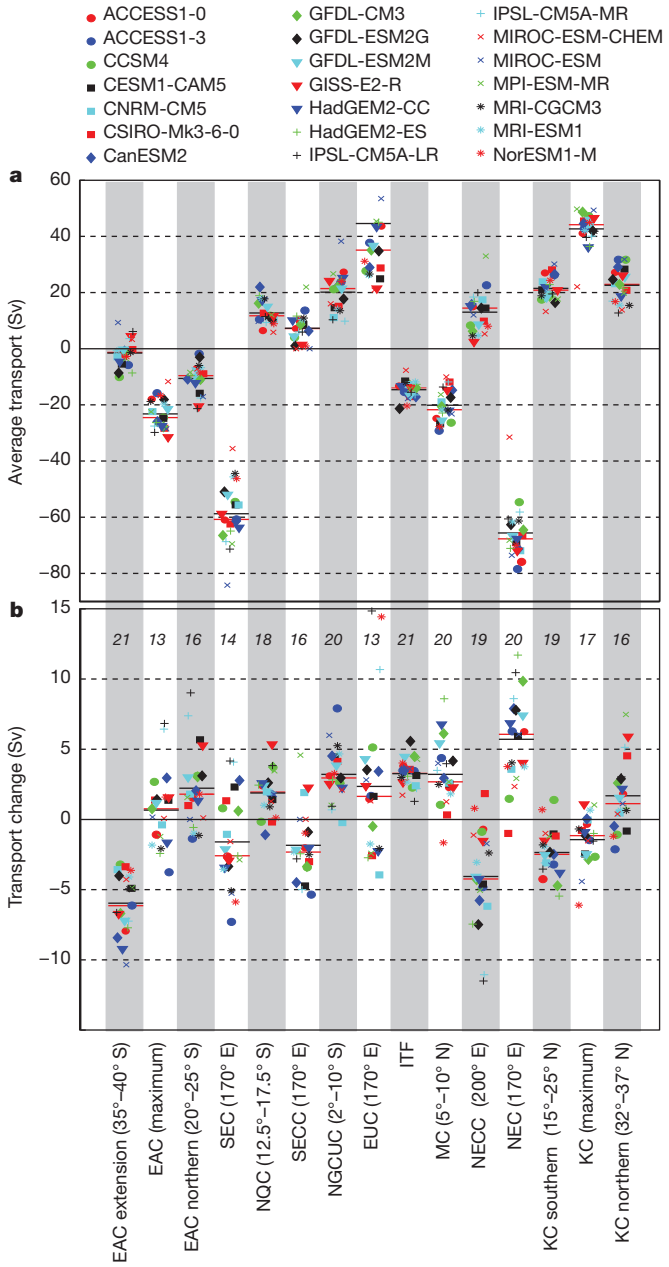

Figure 5 | Modelled transports of annual-mean Pacific WBCs and their projected changes. **a**, Historical mean transport averaged over the twentieth century (positive values indicate northward, and negative, southward transports), and **b**, projected change from the historical mean, averaged over the 2050–2100 period under RCP8.5, for selected Pacific currents (listed at bottom). Positive changes of positive mean transport indicate strengthening, and vice versa. Shown are individual models (markers; see key at top), multi-model mean (horizontal black lines) and multi-model medians (horizontal red lines). Values at the top of each column in **b** indicate the number of models (out of a total of 21) that agree on the sign of the change. Based on a binomial distribution, agreement of 13, 14, 15 and 16 models (out of 21) corresponds to significance levels of 81%, 90.5%, 96% and 99%, respectively. Mean EUC transports for IPSL-CM5A-MR/LR and CNRM-CM5 are greater than 90 Sv, and are not shown in **a**.

Undercurrent, reaches east of the Luzon northern tip[19], or directs eastward between 10°–12° N under the NEC[24,28]. Without such ground-truth information, our confidence in model performance will remain low.

With a sustained community effort, our understanding of the Pacific WBCs and their impacts will continue to improve. The ultimate goal is to produce a reliable projection of the Pacific WBCs and their climatic impacts that is consistent with our physical theoretical understanding, as well as with what observations show. To this end, coordinated observations, studies of processes, and modelling should be bolstered. Our models need to resolve the complex terrain of marginal seas and the detailed structure of the WBCs, together with bathymetry, mesoscale eddies, and other currently unresolved processes, especially turbulent mixing. An international WBC intermodel comparison project may offer a good avenue for a substantial advance. These modelling efforts need to be supported by a coordinated observation system integrating high-density mooring arrays across all Pacific WBCs, satellite observations, Argo floats and platforms that enable near-coast measurements, to provide a three-dimensional picture of the coast-to-deep-water WBC structure. In the meantime, we need to combine all sources of information to make reliable predictions of variability and robust assessments of the response of the Pacific WBCs to greenhouse warming and the associated climatic impacts.

Received 13 August 2014; accepted 8 April 2015.

1. Nakamura, H., Sampe, T., Tanimoto, Y. & Shimpo, A. Observed associations among stormtracks, jet streams and midlatitude oceanic fronts. *AGU Geophys. Monogr. Ser.* **147,** 329–346 (2004).
2. Gordon, A. L. Interocean exchange of thermocline water. *J. Geophys. Res.* **91,** 5037–5046 (1986).
3. Cai, W. *et al.* More extreme swings of the South Pacific convergence zone due to greenhouse warming. *Nature* **488,** 365–369 (2012).
4. Ridgway, K. R. & Dunn, J. R. Observational evidence for a Southern Hemisphere oceanic supergyre. *Geophys. Res. Lett.* **34,** L13612 (2007).
5. Cai, W. Antarctic ozone depletion causes an intensification of the Southern Ocean super-gyre circulation. *Geophys. Res. Lett.* **33,** L03712 (2006).
6. Speich, S., Blanke, B. & Cai, W. Atlantic meridional overturning circulation and the Southern Hemisphere supergyre. *Geophys. Res. Lett.* **34,** L23614 (2007).
7. Hu, D. *et al. Northwestern Pacific Ocean Circulation and Climate Experiment (NPOCE) Science/Implementation Plan* (China Ocean Press, 2011).
   Details of NPOCE, outlining its goal and scope with a comprehensive literature review on ocean circulation and climate in the northwestern Pacific Ocean.
8. Ganachaud, A. S. *et al.* The Southwest Pacific Ocean Circulation and Climate Experiment (SPICE). *J. Geophys. Res.* **119,** 2642–2657 (2014).
9. Gordon, A. L. *et al.* The Indonesian Throughflow during 2004–2006 as observed by the INSTANT program. *Dyn. Atmos. Oceans* **50,** 115–128 (2010).
10. McCreary, J. P. & Lu, P. On the interaction between the subtropical and the equatorial ocean circulations: the subtropical cell. *J. Phys. Oceanogr.* **24,** 466–497 (1994).
11. Gu, D. F. & Philander, S. G. H. Interdecadal climate fluctuations that depend on exchanges between the tropics and extratropics. *Science* **275,** 805–807 (1997).
12. Stommel, H. & Yoshida, K. (eds) *Kuroshio – Its Physical Aspects* (Univ. Tokyo Press, 1972).
13. Gordon, A. L., Flament, P., Villanoy, C. & Centurioni, L. The nascent Kuroshio of Lamon Bay. *J. Geophys. Res.* **119,** 4251–4263 (2014).
14. Burrage, D. Naming a western boundary current from Australia to the Solomon Sea. *CLIVAR Newsl. Exchanges* 58, 28, http://www.clivar.org/node/238 (2012).
15. Kessler, W. S. & Gourdeau, L. The annual cycle of circulation of the south-west subtropical Pacific, analysed in an ocean GCM. *J. Phys. Oceanogr.* **37,** 1610–1627 (2007).
16. Lindstrom, E. *et al.* The western equatorial Pacific Ocean circulation study. *Nature* **330,** 533–537 (1987).
17. Gordon, A. & Fine, R. Pathways of water between the Pacific and Indian oceans in the Indonesian seas. *Nature* **379,** 146–149 (1996).
18. Fine, R. A., Lukas, R., Bingham, F. M., Warner, M. J. & Gammon, R. H. The western equatorial Pacific is a water mass crossroads. *J. Geophys. Res.* **99,** 25063–25080 (1994).
19. Johnson, G., Sloyan, B., Kessler, W. & McTaggart, K. Direct measurements of upper ocean currents and water properties across the tropical Pacific during the 1990s. *Prog. Oceanogr.* **52,** 31–61 (2002).
20. Gouriou, Y. & Toole, J. Mean circulation of the upper layers of the western equatorial Pacific Ocean. *J. Geophys. Res.* **98,** 22495–22520 (1993).
21. Hu, D. & Cui, M. The western boundary current of the Pacific and its role in the climate. *Chin. J. Oceanology Limnol.* **9,** 1–14 (1991).
22. Qu, T., Kagimoto, T. & Yamagata, T. A subsurface countercurrent along the east coast of Luzon. *Deep Sea Res. Part I* **44,** 413–423 (1997).
23. Hu, D. *et al.* Direct measurements of the Luzon Undercurrent. *J. Phys. Oceanogr.* **43,** 1417–1425 (2013).
24. Lukas, R. *et al.* Observations of the Mindanao Current during the Western Equatorial Pacific Ocean Circulation study (WEPOCS). *J. Geophys. Res.* **96,** 7089–7104 (1991).
25. Qu, T. & Lindstrom, E. J. Northward Intrusion of Antarctic Intermediate Water in the Western Pacific. *J. Phys. Oceanogr.* **34,** 2104–2118 (2004).
26. Zhang, L., Hu, D., Hu, S., Wang, F. & Yuan, D. Mindanao Current/Undercurrent measured by a subsurface mooring. *J. Geophys. Res. Oceans* **119,** 3617–3628 (2014).
    Confirms the existence of the Mindanao Undercurrent and reveals its strong 60–80-day variability using observations spanning two years.

27. Wijffels, S., Firing, E. & Toole, J. The mean structure and variability of the Mindanao Current at 8°N. *J. Geophys. Res.* **100,** 18421–18435 (1995).
28. Kashino, Y., Ishida, A. & Kuroda, Y. Variability of the Mindanao Current: mooring observation results. *Geophys. Res. Lett.* **32,** L18611 (2005).
29. Firing, E., Kashino, Y. & Hacker, P. Energetic subthermocline currents observed east of Mindanao. *Deep Sea Res. Part II* **52,** 605–613 (2005).
30. Kessler, W. S. & Cravatte, S. ENSO and short-term variability of the south equatorial current entering the Coral Sea. *J. Phys. Oceanogr.* **43,** 956–969 (2013).
31. Davis, R. E., Kessler, W. S. & Sherman, J. T. Gliders measure western boundary current transport from the South Pacific to the equator. *J. Phys. Oceanogr.* **42,** 2001–2013 (2012).
32. Gasparin, F., Ganachaud, A., Maes, C., Marin, F. & Eldin, G. Oceanic transports through the Solomon Sea: the bend of the New Guinea Coastal Undercurrent. *Geophys. Res. Lett.* **39,** L15608 (2012).
A hydrographic survey across the southern Solomon Sea allows a complete estimate of the NGCU transports down to 2,000 m, as well as counter currents, inflows and outflows between the Solomon and Coral Seas.
33. Qu, T. & Lindstrom, E. A climatological interpretation of the circulation in the western South Pacific. *J. Phys. Oceanogr.* **32,** 2492–2508 (2002).
34. Qu, T. & Lukas, R. The bifurcation of the North Equatorial Current in the Pacific. *J. Phys. Oceanogr.* **33,** 5–18 (2003).
First report of the findings of vertical distribution and seasonal variation of the NEC bifurcation, with strong relevance to seasonal variation of the South China Sea throughflow in the Luzon Strait found by later studies.
35. Qiu, B. & Lukas, R. Seasonal and interannual variability of the North Equatorial Current, the Mindanao Current and the Kuroshio along the Pacific western boundary. *J. Geophys. Res.* **101,** 12315–12330 (1996).
36. Ridgway, K. R. Long term trend and decadal variability of the southward penetration of the East Australia Current. *Geophys. Res. Lett.* **34,** L13613 (2007).
37. Roemmich, D. *et al.* Decadal spinup of the South Pacific Subtropical Gyre. *J. Phys. Oceanogr.* **37,** 162–173 (2007).
38. Beal, L. M. On the role of the Agulhas system in ocean circulation and climate. *Nature* **472,** 429–436 (2011).
39. Qiu, B., Mao, M. & Kashino, Y. Intraseasonal variability in the Indo-Pacific throughflow and the regions surrounding the Indonesian seas. *J. Phys. Oceanogr.* **29,** 1599–1618 (1999).
40. Kim, Y. *et al.* Seasonal and interannual variations of the North Equatorial Current bifurcation in a high-resolution OGCM. *J. Geophys. Res.* **109,** C03040 (2004).
41. Kashino, Y. *et al.* Observations of the North Equatorial Current, Mindanao Current, and the Kuroshio Current system during the 2006/7 El Niño and 2007/08 La Niña. *J. Oceanogr.* **65,** 325–333 (2009).
42. Qiu, B. & Chen, S. Interannual-to-decadal variability in the bifurcation of the north equatorial current off the Philippines. *J. Phys. Oceanogr.* **40,** 2525–2538 (2010).
Shows a decadal modulation in the characteristics of the NEC bifurcation, which is determined by wind forcing in the 12°–14° N band that contains variability not fully representable by the Niño-3.4 index.
43. Wu, C.-R. Interannual modulation of the Pacific Decadal Oscillation (PDO) on the low-latitude western North Pacific. *Prog. Oceanogr.* **110,** 49–58 (2013).
44. Qiu, B., Kessler, W. S. & Chen, S. Source of the 70-day mesoscale eddy variability in the Coral Sea and North Fiji Basin. *J. Phys. Oceanogr.* **39,** 404–420 (2009).
45. Ueki, I., Kashino, Y. & Kuroda, Y. Observation of current variations off the New Guinea coast including the 1997–1998 El Niño period and their relationship with Sverdrup transport. *J. Geophys. Res.* **108** (C7), 3243 (2003).
46. Jin, F. F. An equatorial ocean recharge paradigm for ENSO. Part I: conceptual model. *J. Atmos. Sci.* **54,** 811–829 (1997).
47. Melet, A., Gourdeau, L., Verron, J. & Djath, B. Solomon Sea circulation and water mass modifications: response at ENSO timescales. *Ocean Dyn.* **63,** 1–19 (2013).
48. Sprintall, J. *et al.* The Indonesian seas and their role in the coupled ocean–climate system. *Nature Geosci.* **7,** 487–492 (2014).
Reports recent progress in our understanding of oceanography in the Indonesian Seas and their climatic impact through variations with ENSO, focusing on ocean heat content, sea level, winds and precipitation in the tropical Indian Ocean region.
49. van Sebille, E. *et al.* Pacific-to-Indian Ocean connectivity: Tasman leakage, Indonesian Throughflow, and the role of ENSO. *J. Geophys. Res. Oceans* **119,** 1365–1382 (2014).
50. Gordon, A. L. *et al.* South China Sea throughflow impact on the Indonesian throughflow. *Geophys. Res. Lett.* **39,** L11602 (2012).
51. Qu, T., Yan, D. & Hideharu, S. South China Sea throughflow: a heat and freshwater conveyor. *Geophys. Res. Lett.* **33,** L23617 (2006).
52. Hill, K. L., Rintoul, S. R., Ridgway, K. R. & Oke, P. R. Decadal changes in the South Pacific western boundary current system revealed in observations and ocean state estimates. *J. Geophys. Res.* **116,** C01009 (2011).
53. Vecchi, G. A. *et al.* Weakening of tropical Pacific atmospheric circulation due to anthropogenic forcing. *Nature* **441,** 73–76 (2006).
54. Kelly, K. A. *et al.* Western boundary currents and frontal air–sea interaction: Gulf Stream and Kuroshio Extension. *J. Clim.* **23,** 5644–5667 (2010).
55. Kwon, Y. O. *et al.* Role of the Gulf Stream and Kuroshio–Oyashio systems in large-scale atmosphere–ocean interaction: a review. *J. Clim.* **23,** 3249–3281 (2010).
56. Konda, M. H., Ichikawa, H., Tomita, H. & Cronin, M. F. Surface heat flux variations across the Kuroshio Extension as observed by surface flux buoys. *J. Clim.* **23,** 5206–5221 (2010).
57. Chelton, D. B., Schlax, M., Freilich, M. & Milliff, R. Satellite measurements reveal persistent small-scale features in ocean winds. *Science* **303,** 978–983 (2004).
58. Tokinaga, H. *et al.* Ocean frontal effects on the vertical development of clouds over the western North Pacific: *in situ* and satellite observations. *J. Clim.* **22,** 4241–4260 (2009).
59. Hotta, D. & Nakamura, H. On the significance of the sensible heat supply from the ocean in the maintenance of the mean baroclinicity along storm tracks. *J. Clim.* **24,** 3377–3401 (2011).
60. Wu, C.-R. *et al.* Air-sea interaction between tropical cyclone Nari and Kuroshio. *Geophys. Res. Lett.* **35,** L12605 (2008).
61. Sasaki, n., Minobe, S., Asai, T. & Inatsu, M. Influence of the Kuroshio in the East China Sea on the early summer (baiu) rain. *J. Clim.* **25,** 6627–6645 (2012).
62. Huang, R. & Li, W. Influence of the heat source anomaly over the tropical western Pacific on the subtropical high over East Asia and its physical mechanism. *Chinese J. Atmos. Sci.* **14,** 95–107 (1988).
63. Feng, J. & Hu, D. How much does heat content of the western tropical Pacific Ocean modulate the South China Sea summer monsoon onset in the last four decades? *J. Geophys. Res. Oceans* **119,** 4029 (2014).
64. Holland, G. J. Interannual variability of the Australian summer monsoon at Darwin: 1952–82. *Mon. Weath. Rev.* **114,** 594–604 (1986).
65. Gordon, A. L., Susanto, R. D. & Vranes, K. Cool Indonesian throughflow as a consequence of restricted surface layer flow. *Nature* **425,** 824–828 (2003).
Shows that a stronger low-salinity South China Sea throughflow during boreal winter sets up a gradient, which limits the Mindanao Current inflow into the Indonesian Seas and thus leads to cold surface water in the Indonesian Seas.
66. Seager, R., Kushnir, Y., Naik, N. H., Cane, M. A. & Miller, J. Wind-driven shifts in the latitude of the Kuroshio–Oyashio Extension and generation of SST anomalies on decadal timescales. *J. Clim.* **14,** 4249–4265 (2001).
67. Lau, N.-C. & Nath, M. J. Impact of ENSO on SST variability in the North Pacific and North Atlantic: seasonal dependence and role of extratropical sea–air coupling. *J. Clim.* **14,** 2846–2866 (2001).
68. Alexander, M. A. The atmospheric bridge: the influence of ENSO teleconnections on air–sea interaction over the global oceans. *J. Clim.* **15,** 2205–2231 (2002).
69. Nakamura, H. & Kazmin, A. S. Decadal changes in the North Pacific oceanic frontal zones as revealed in ship and satellite observations. *J. Geophys. Res.* **108,** 3078 (2003).
70. Taguchi, B. *et al.* Decadal variability of the Kuroshio Extension: observations and an eddy-resolving model hindcast. *J. Clim.* **20,** 2357–2377 (2007).
71. Frankignoul, C. & Sennéchael, N. Observed influence of North Pacific SST anomalies on the atmospheric circulation. *J. Clim.* **20,** 592–606 (2007).
72. Taguchi, B., Nakamura, H., Nonaka, M. & Xie, S.-P. Influences of the Kuroshio/Oyashio Extensions on air–sea heat exchanges and storm-track activity as revealed in regional atmospheric model simulations for the 2003/04 cold season. *J. Clim.* **22,** 6536–6560 (2009).
73. Taguchi, B., Xie, S.-P., Mitsudera, H. & Kubokawa, A. Response of the Kuroshio Extension to Rossby waves associated with the 1970s climate regime shift in a high-resolution ocean model. *J. Clim.* **18,** 2979–2995 (2005).
74. Liu, Z. & Alexander, M. Atmospheric bridge, oceanic tunnel and global climatic teleconnections. *Rev. Geophys.* **45,** RG2005 (2007).
75. Tokinaga, H. *et al.* Atmospheric sounding over the winter Kuroshio Extension: effect of surface stability on atmospheric boundary layer structure. *Geophys. Res. Lett.* **33,** L04703 (2006).
76. Norris, J. R. & Leovy, C. B. Interannual variability in stratiform cloudiness and sea surface temperature. *J. Clim.* **7,** 1915–1925 (1994).
77. Klein, S. A., Hartmann, D. L. & Norris, J. R. On the relationships among low-cloud structure, sea surface temperature and atmospheric circulation in the summertime northeast Pacific. *J. Clim.* **8,** 1140–1155 (1995).
78. Park, S., Alexander, M. A. & Deser, C. The impact of cloud radiative feedback, remote ENSO forcing, and entrainment on the persistence of North Pacific sea surface temperature anomalies. *J. Clim.* **19,** 6243–6261 (2006).
79. Alexander, M. A. & Deser, C. A mechanism for the recurrence of wintertime midlatitude SST anomalies. *J. Phys. Oceanogr.* **25,** 122–137 (1995).
80. Sugimoto, S. & Hanawa, K. Remote reemergence areas of winter sea surface temperature anomalies in the North Pacific. *Geophys. Res. Lett.* **32,** L01606 (2005).
81. Nakamura, H. & Yamagata, T. in *Beyond El Nino: Decadal and Interdecadal Climate Variability* (ed. Navarra, A.) 49–72 (Springer, 1999).
82. Sprintall, J., Roemmich, D., Stanton, B. & Bailey, R. Regional climate variability and ocean heat transport in the southwest Pacific Ocean. *J. Geophys. Res.* **100,** 15865–15871 (1995).
83. Shi, G., Ribbe, J., Cai, W. & Cowan, T. An interpretation of Australian rainfall projections. *Geophys. Res. Lett.* **35,** L02702 (2008).
84. Godfrey, S. The effect of the Indonesian Throughflow on ocean circulation and heat exchange with the atmosphere: A review. *J. Geophys. Res. Oceans* **101,** 12217–12237 (1996).
85. Vranes, K., Gordon, A. L. & Field, A. The heat transport of the Indonesian throughflow and implications for the Indian Ocean heat budget. *Deep Sea Res. Part II* **49,** 1391–1410 (2002).
86. Gordon, A. L. Oceanography of the Indonesian Seas and their throughflow. *Oceanography (Wash. D.C.)* **18,** 14–27 (2005).
87. Song, Q., Gordon, A. L. & Visbeck, M. Spreading of the Indonesian throughflow in the Indian Ocean. *J. Phys. Oceanogr.* **34,** 772–792 (2004).
88. Wu, L. *et al.* Enhanced warming over the global subtropical western boundary current. *Nature Clim. Change* **2,** 161–166 (2012).
Demonstrates synchronized enhanced warming along subtropical WBCs and emphasizes the important roles played by the WBCs in global climate change.
89. Zhai, F., Hu, D., Wang, Q. & Wang, F. Long-term trend of Pacific South Equatorial Current bifurcation. *Geophys. Res. Lett.* **41,** 3172–3180 (2014).
90. Chen, Z. & Wu, L. Long-term change of the Pacific North Equatorial Current bifurcation in SODA. *J. Geophys. Res.* **117,** C06016 (2012).

91. Cai, W. & Cowan, T. Trends in Southern Hemisphere circulation in IPCC AR4 models over 1950–1999: ozone-depletion vs greenhouse forcing. *J. Clim.* **20,** 681–693 (2007).
92. Cai, W., Shi, G., Cowan, T., Bi, D. & Ribbe, J. The response of the Southern Annular Mode, the East Australian Current, and the southern mid-latitude ocean circulation to global warming. *Geophys. Res. Lett.* **32,** L23706 (2005).
93. Thompson, D. W. J. *et al.* Signatures of the Antarctic ozone hole in Southern Hemisphere surface climate change. *Nature Geosci.* **4,** 741–749 (2011).
94. Wang, G., Cai, W. & Purich, A. Trends in Southern Hemisphere wind driven circulation in CMIP5 models over the 21st century: ozone recovery versus greenhouse forcing. *J. Geophys. Res. Oceans* **119,** 2974–2986 (2014).
95. Ganachaud, A. *et al.* Projected changes in the tropical Pacific Ocean of importance to tuna fisheries. *Clim. Change* **119,** 163–179 (2013).
Presents global warming projections showing a shift in the Pacific winds and surface temperatures that affect oceanic currents and vertical ocean structure, enhancing stratification and increasing the extent of the warm pool with consequences for tuna habitat.
96. Sen Gupta, A., Ganachaud, A., McGregor, S., Brown, J. N. & Muir, L. Drivers of the projected changes to the Pacific Ocean equatorial circulation. *Geophys. Res. Lett.* **39,** L09605 (2012).
97. Grenier, M., Jeandel, C. & Cravatte, S. From the subtropics to the equator in the Southwest Pacific: continental material fluxes quantified using neodymium data along modelled thermocline water pathways. *J. Geophys. Res. Oceans* **119,** 3948–3966 (2014).
98. Gregory, J. M. *et al.* A model intercomparison of changes in the Atlantic thermohaline circulation in response to increasing atmospheric CO_2 concentration. *Geophys. Res. Lett.* **32,** L12703 (2005).
99. Li, W., Li, L., Ting, M. & Liu, Y. Intensification of Northern Hemisphere subtropical highs in a warming climate. *Nature Geosci.* **5,** 830–834 (2012).
100. Oliver, E. C. J. & Holbrook, N. J. Extending our understanding of South Pacific gyre "spin-up": modeling the East Australian Current in a future climate. *J. Geophys. Res. Oceans* **119,** 2788–2805 (2014).
Shows that an increase in the EAC extension of 4–5 Sv by 2060 simulated by a high-resolution model closely matches results from a low-resolution climate model.

Acknowledgements W.C. and G.W. are supported by the Australian Climate Change Science Program, a CSIRO Office of the Chief Executive Science Leader award, and CSIRO Office of the Chief Executive postdoctoral awards. L.W., Z.C. and X.L. are supported by projects (41130859,41490640, 41306001) of the National Science Foundation of China (NSFC), and a project (2013CB956200) of the National Basic Research Program of China (MOST). D.H. is supported by CAS Program XDA 11010101, and NSFC Grants 41330963 and 41421005. S.H. is supported by NSFC Grant 41406016. Q.W. is supported by MOST Grant 2013CB956202. F.W. is supported by MOST Grant 2012CB417401 and NSFC/Shangdong Grant U1406401, A.G. is supported by CNRS/INSU/LEFE project MoorSPICE. This is PMEL Contribution Number 4207, and Lamont-Doherty Earth Observatory Contribution Number 7875. J.S. is supported by the National Aeronautics and Space Administration (NASA) under award no. NNX13AO38G. Y.K. is supported by the Tropical Ocean Climate Study of Japan Agency for Marine-Earth Science and Technology. This is a contribution to the CLIVAR SPICE and NPOCE programmes. We thank A. Purich and T. Cowan for their comments before submission. We acknowledge the World Climate Research Programme's Working Group on Coupled Modelling, and we thank the climate modelling groups for producing and making available their model output. The US Department of Energy's Program for Climate Model Diagnosis and Intercomparison provides coordinating support and led the development of software infrastructure in partnership with the Global Organization for Earth System Science Portals.

Author Contributions D.H., L.W. and W.C. conceived the study. L.W., W.C. and D.H. determined the scope. W.C. wrote the draft of the paper and finalized the manuscript with help from G.W. A.S.G. conducted model output analysis for future projections and plotted Fig. 5. A.G., A.S.G. and W.C. constructed the schematic of Figs 1 and 3. Z.C. generated Fig. 4. All authors contributed to interpreting results, discussion of the associated dynamics and improvement of this paper.

Author Information Reprints and permissions information is available at www.nature.com/reprints. The authors declare no competing financial interests. Readers are welcome to comment on the online version of the paper. Correspondence and requests for materials should be addressed to W.C. (wenju.cai@csiro.au) or L.W. (lxwu@ouc.edu.cn).